

Evolution of the Diurnal Cycle of Tropical Rainfall associated with the Madden-Julian Oscillation

LEANNE BLIND-DOSKOCIL*

*National Weather Center Research Experiences for Undergraduates Program
Norman, Oklahoma*

NAOKO SAKAEDA

*School of Meteorology, University of Oklahoma
Norman, OK*

ABSTRACT

This study evaluates the impact of the Madden-Julian oscillation on the diurnal cycle of tropical rainfall and cloud populations by analyzing data from the TOGA radar aboard R/V Roger Revelle. The data was collected during the DYNAMO field campaign which investigated MJO initiation processes and cloud evolution. Rain rate and rain type data were examined to understand the diurnal cycle observed by the TOGA radar. The mean hourly time series of rainfall during the overall field campaign displayed a strong afternoon maximum in comparison to the climatological diurnal cycle that has been documented by satellite-based rain estimates. The diurnal cycle during the MJO enhanced phase shows a strong afternoon maximum when compared to S-PolKa radar. Large differences were observed in the time series of the diurnal cycles between the two MJO events that occurred during the observed period. This study aims to increase knowledge of the diurnal cycle with respect to the MJO by studying differences seen between the TOGA and S-PolKa radars.

1. Introduction

The Madden-Julian oscillation (MJO) plays a significant role in how rainfall and cloud populations evolve on subseasonal to seasonal timescales within the tropics. The MJO has implications on other meteorological phenomenon such as monsoons, tropical cyclones, El Niño-Southern Oscillation, and jet stream patterns (e.g., Gottschalck 2014). As the MJO and tropical rainfall are important components of the climate system, studying tropical rainfall will help improve climate models to improve climate prediction (Rockwell 2012). To improve the representation of the MJO in climate models, it is key to develop our understanding of its interactions with clouds, and the diurnal cycle is one of the fundamental variabilities of cloudiness and rainfall. Advancement in understanding the MJO and how it impacts the diurnal cycle of rainfall and cloud populations will provide more insight into predicting MJO events and understanding tropical rainfall.

The Madden-Julian oscillation was first discovered by two scientists, Roland Madden and Paul Julian, in 1971. They observed an eastward propagating intraseasonal dis-

tribution of clouds, rainfall, pressure changes, and wind speeds in the tropics (Madden and Julian 1971). The MJO occurs on a timescale of 30-90 days and modulates convective activity over zonal widths of 12,000 to 20,000 km. These envelopes of anomalous convective activity then propagate eastward from the Indian Ocean into the Pacific Ocean (Zhang 2005). The oscillation involves convectively enhanced and suppressed regions, which are referred to as enhanced and suppressed phases throughout this manuscript. The enhanced phase is associated with anomalous surface convergence and divergence aloft that drive upward motion; this upward motion enhances deep convection and rainfall in this region. The opposite happens in the suppressed phase where anomalous surface divergence and descending air suppress overall convection and rainfall. Cloud populations in the enhanced phase are more widespread and organized while isolated convection and scattered cloud types dominate in the suppressed phase (Xu and Rutledge 2014). MJO initiation is hypothesized to be contributed by surface heat fluxes, radiative destabilization, dynamically-forced ascent through surface wind convergence or upper-level divergence, modulation of the thermocline through oceanic waves, the amount and timing of lower tropospheric moisture, and moistening by cumulus clouds (Yoneyama et al. 2013).

*Corresponding author address: Leanne Blind-Doskocil, Texas A&M University 3150 TAMU College Station, Texas 77843-3150
E-mail: leanneblind@gmail.com

The DYNAMO field campaign (Dynamics of the Madden-Julian Oscillation) took place from October 2011 to March 2012 to collect data for the primary reason of studying the MJO initiation processes and cloud evolution. The campaign aimed to improve knowledge about the MJO to enhance its prediction and improve cloud parameterizations for general circulation models (Yoneyama et al. 2013). Data were collected from multiple sources including deploying radars on land/atolls and ships, acquiring measurements from buoys, and releasing dropsondes from aircraft. Some radars deployed during the campaign include S-PolKa and SMART-R on Addu Atoll and TOGA (Tropical Ocean-Global Atmosphere) and Mirai radars on ships; these radars provide high-resolution, three-dimensional data on precipitating clouds. Wind speed and direction at different heights, sea surface temperature, outgoing longwave radiation, reflectivity, and temperature profiles were monitored during the campaign. Most of the campaign happened over the Indian Ocean and the Maritime Continent, but the whole campaign extended from East Africa to the western Pacific (Gottschalck et al. 2013).

To better understand tropical rainfall, it is important to analyze different cloud types and their evolutions to monitor the effects on the atmosphere from different latent heating profiles, reflectivities, instabilities, etc. Studying the diurnal cycle of cloud populations and tropical rainfall is fundamental to examining cloud processes. This study investigates the effect of the MJO on the diurnal cycle of tropical cloud evolution and rainfall. As shown by Sakaeda et al. (2017) and Oh et al. (2012), the climatological diurnal cycle of tropical rainfall over the ocean displays an early morning maximum in rainfall around 0000-0600 LST. This contrasts the late afternoon peak in rainfall usually observed over land. Several hypotheses exist for why this happens including the effects of radiational cooling, enhanced low-level convergence, the amount/timing of lower tropospheric moisture, and the life cycles of mesoscale convective systems (Sakaeda et al. 2018). The cloud types evolve during the early morning peak from deep convective rain to stratiform rain as the peak starts to dissipate. Sakaeda et al. (2018) studied the differences in the diurnal cycle between the MJO enhanced and suppressed phases using the S-PolKa radar. The study observed an early morning maximum in rainfall around 0600 LST during the enhanced phase with a greater magnitude in total rainfall when compared to the suppressed phase. Two peaks in rainfall were noted in the suppressed phase during the early morning hours (0300 LST) and the late afternoon hours (1800 LST). Compared to the enhanced phase, isolated convective precipitation was observed the most along with less mean rainfall during the suppressed phase.

However, Sakaeda et al. (2018) only analyzed the diurnal cycle of rainfall and cloud populations with respect

to the S-PolKa radar, which collected data over a limited spatiotemporal domain. To further this study, this paper investigates the diurnal cycle using data from the TOGA radar that was deployed on the ship R/V Roger Revelle about 800 km east of S-Polka. This study will also examine differences in the diurnal cycle within the MJO enhanced and suppressed phases and its variations among the different MJO events observed. The following questions will be discussed in this paper:

1. How do the daily and diurnal cycles of tropical rainfall evolve based on the TOGA radar?
2. Does the TOGA radar show the same changes in the diurnal cycle associated with the MJO enhanced and suppressed phases as Sakaeda et al. (2018)?

2. Data and Methods

a. Radar

Radar data used for this project was collected by the DYNAMO field campaign. This study uses data that was collected by the TOGA radar onboard the ship R/V Roger Revelle during the field campaign (Fig. 1). TOGA is a C-band radar operating on a 5 cm wavelength; S-PolKa, comparatively, had a wavelength of 10 cm. TOGA radar was operated mostly in the Indian Ocean south of Sri Lanka and east of the Maldives at 0° , 80.5°E (Xu and Rutledge 2014). TOGA had a scanning radius of 150 km and made a full volume scan every 10 minutes. TOGA scanned five vertical cross sections with elevation angles 0.8° to 40° and 22 plan position indicator sweeps in FAR and NEAR modes with elevation angles of 0.8° to 21.5° and 0.8° to 35.9° respectively (Xu and Rutledge 2014). The majority of the time TOGA was not collecting data happened during the suppressed phases of the MJO. Table 1 displays the time periods when Revelle was at sea collecting data and when it was positioned at the station location (Xu and Rutledge 2014). For this study, only the time periods involving cruises two (2-29 Oct 2011) and three (9 Nov-5 Dec 2011) at the station are investigated which overlap with the first and second MJO events observed during the field campaign. This study will look at the diurnal cycle variability between the S-PolKa and TOGA radars.

TABLE 1. Cruise dates for the TOGA radar during the DYNAMO field campaign. Cruises 2 and 3 are evaluated for this study.

	Cruise 2 (MJO Event 1)	Cruise 3 (MJO Event 2)
Cruise Time	30 Sep-1 Nov 2011	7 Nov-10 Dec 2011
Time around 0° , 80.5°E	2-29 Oct 2011	9 Nov-5 Dec 2011

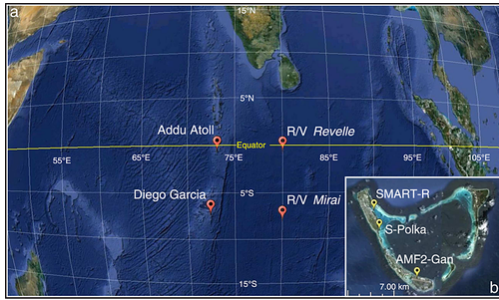


FIG. 1. Locations of TOGA radar located on R/V Revelle and S-PolKa radar located on Addu Atoll during the DYNAMO field campaign (From Powell and Houze Jr. 2013).

b. Radar initial and derived products

The radar reflectivity data was transformed into rain rate and rain type data, which is available through the DYNAMO Legacy website at http://dynamo.ml-ext.ucar.edu/dynamo_legacy/. The best rain rate estimates were derived using the reflectivity at the 2.5 km level. The data also include rain rate minimums and maximums that provide estimates on uncertainty and error in measurements. Rain rate and rain type data are available at every 10 minute and 1 km horizontal resolution. Algorithms proposed by Powell et al. (2016) classified rainfall into six types: stratiform, convective, uncertain (combination of convective and stratiform), isolated convective core, isolated convective fringe, and weak. The method for classifying rain type uses the lowest scan angle of reflectivity to more accurately represent precipitation at the surface instead of interpolating radar data at a constant height (Powell et al. 2016). Using this method, embedded and shallow convective rain in stratiform precipitation, weak echoes, and shallow isolated precipitation are more accurately depicted. These products are explored to understand the contributions of cloud types on the diurnal cycle.

c. Classification of MJO phases

The MJO phases are identified in the same manner as Sakaeda et al. (2018). This method uses 2.5 horizontal resolution and daily outgoing longwave radiation (OLR) that is filtered for MJO wavenumber-frequency band (20-100 days, 1-5 eastward zonal wavenumbers) averaged over a 5° box around the location of Revelle; this is then used to identify each day during the campaign as enhanced phase, suppressed phase, or neither. Days with the MJO-filtered OLR anomaly below the lower-15th-percentile threshold value are classified as enhanced phase and days above the upper-15th-percentile threshold value are classified as suppressed phase.

d. Composite analysis

Rain rate estimates from TOGA radar are averaged during the entire DYNAMO period and during the MJO enhanced and suppressed phases to study the overall diurnal cycle and its changes with the MJO. For this study, only data from days that corresponded to cruise periods 2 and 3 at the station (0°, 80.5°E) were analyzed for each MJO phase. Table 2 outlines the days that correspond to each cruise period at the station and the MJO phase.

TABLE 2. Dates of MJO enhanced and suppressed phases from TOGA radar that are used in this study.

	Enhanced Phase	Suppressed Phase
Cruise 2	22-29 Oct 2011	6-17 Oct 2011
Cruise 3	22 Nov-2 Dec 2011	9-19 Nov 2011

Local solar time (LST) is calculated from UTC time by

$$LST = UTC + 24 \cdot \frac{\text{longitude}}{360} \quad (1)$$

where longitude is the number of degrees east of the prime meridian and UTC is in hours. Looking at time relative to the sun is important when examining the effects of diurnal forcing.

3. Results

a. Daily progression of rain rate

The daily progression of rainfall rate is plotted for the TOGA radar while on station (0°, 80.5°E) from October 1 to December 8 (Fig 2.) The gray line shows days with no data collection on October 31, November 1, November 2, November 3, and November 6 and very little data collection on November 4 and 5. Three MJO events were observed during the DYNAMO field campaign, and the first two events took place in October and November 2011; MJO events 1 and 2 observed during cruises 2 and 3 by Revelle are represented by the two sets of MJO suppressed and enhanced phases in Figure 2. The aqua and pink bars highlight the MJO enhanced and suppressed phases, respectively, that occurred during this period (see dates in Table 2).

Daily rainfall amounts tend to be higher within the MJO enhanced phases than the suppressed (Xu and Rutledge 2014; Sakaeda et al. 2018). During the enhanced phases, deep convection and mixed rainfall are the most prevalent types of rainfall with stratiform rain being secondary. The increase in rainfall observed during the enhanced phase is attributed to an increase in stratiform rain. During the suppressed phases, deep convection prevails with isolated convection becoming more prominent than in the enhanced phase. Both suppressed phases have little contribution of stratiform rainfall to the total. Between the MJO

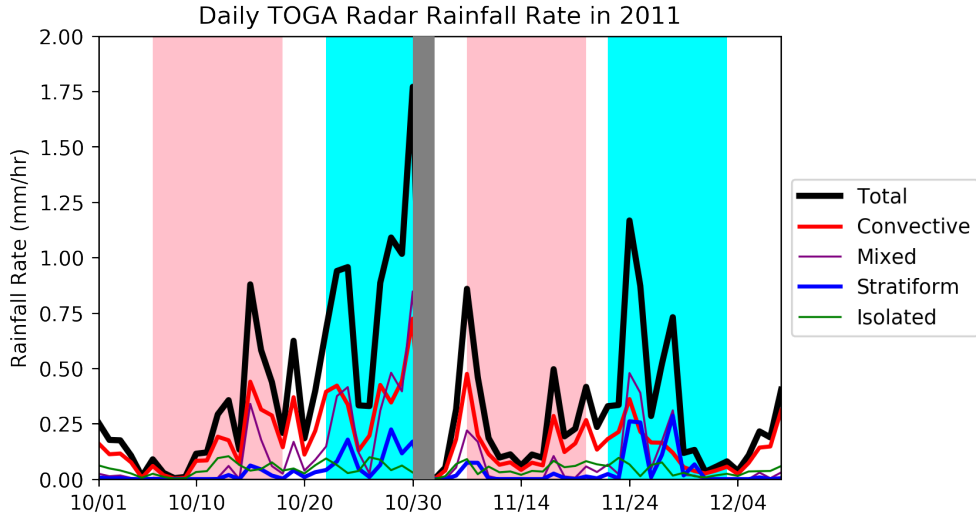


FIG. 2. Daily progression of rainfall rates from the TOGA radar stationed at 0° , 80.5°E from October 1 to December 8. The thick black line shows total precipitation, the red line shows deep convection, the thin purple line shows convection and stratiform mixed, the blue line shows stratiform, and the thin green line shows isolated convection. The aqua and pink bars indicate the MJO enhanced and suppressed phases respectively. The gray line eliminates misrepresentation in data from no data collection on October 31, November 1, November 2, November 3, and November 6 and very little data collection on October 30, November 4, and November 5.

events, stratiform rain contributes more to the total rainfall amount during the enhanced phase of MJO event 2. The largest maximum in rainfall was observed at the end of the enhanced phase in MJO event one similarly to Xu and Rutledge (2014) even though the peak is not observed in other studies that used S-PolKa.

b. Diurnal cycle climatology

Figure 3 shows the mean diurnal cycle of rainfall for TOGA radar, displaying total precipitation and contributions by rain types (Fig. 3). The primary maximum in total rainfall happens between 0000 and 0400 LST. Contrary to Sakaeda et al. (2018) using S-PolKa radar, the TOGA radar observed a secondary peak in rainfall in the afternoon hours around 1600 to 1900 LST. The early morning maximum had the most contributions from deep convection and mixed precipitation that evolves into stratiform rainfall as the morning hours progress. The peak in rainfall in the afternoon starts off as isolated convection that peaks around 1400 LST and transitions into mixed and deep convection around 1600-1900 LST.

c. Diurnal cycle during MJO enhanced and suppressed phases

The mean diurnal cycle of rainfall is separated into the MJO enhanced and suppressed phases (Fig. 4a and 4b). The contributions of each rain type relative to the total rainfall are also separated into the enhanced and suppressed phases (Fig. 4c and 4d).

Two peaks in total rainfall are observed in the enhanced phase; a strong afternoon peak is observed around 1700 to

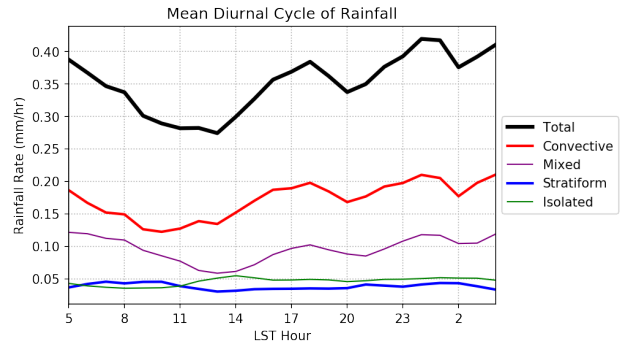


FIG. 3. Mean diurnal cycle of tropical rainfall in local solar time by rain type: total (thick black line), convective (red line), mixed (thin purple line), stratiform (blue line), and isolated (thin green line).

1800 LST with a secondary early morning peak at 0100 LST. Although the amounts of rainfall are similar with these two peaks, different evolutions of rain types contribute to these two peaks. The afternoon peak is generated by isolated convection developing into deep convection and mixed precipitation. Stratiform rainfall does not contribute much to the afternoon maximum; stratiform rainfall contributes to 14% of the total rainfall for the afternoon peak (Fig. 4c). The morning peak is initially contributed by deep convection and evolves into mixed precipitation that later progresses into stratiform rainfall as the peak dwindles. Overall, deep convection and mixed precipitation prevail throughout the enhanced phase diurnal cycle. Deep convection contributes to 39% of the total rainfall and mixed rainfall contributes to 35% (Fig. 4c).

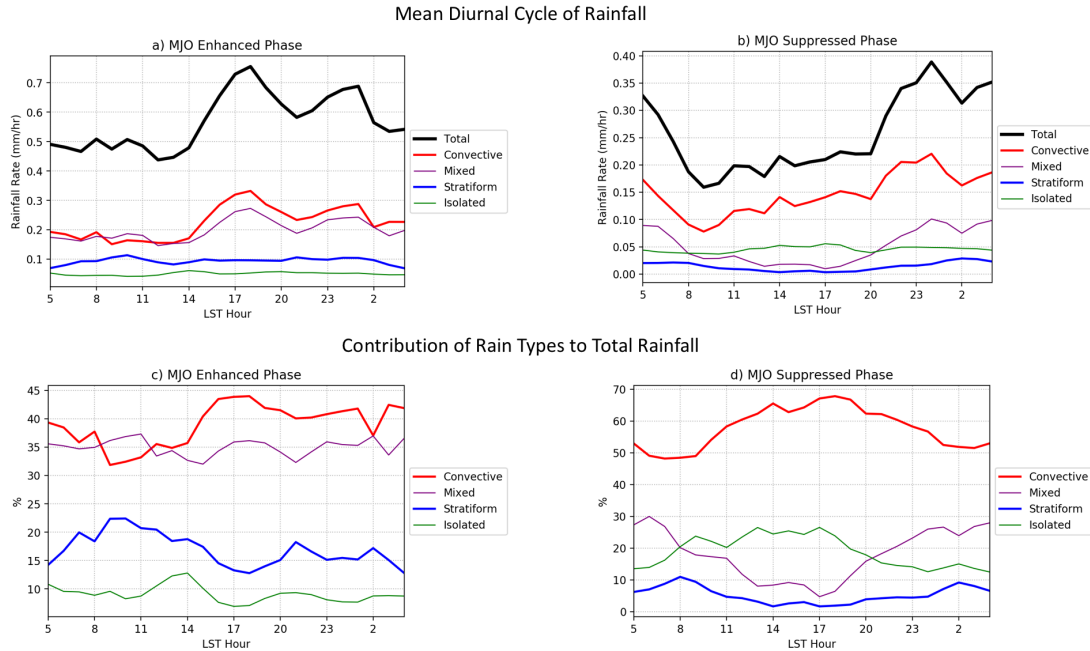


FIG. 4. Mean diurnal cycle of rainfall separated by (a) MJO enhanced and (b) suppressed phases from TOGA. The contributions of each rain type to the total rainfall are also separated by the (c) MJO enhanced and (d) suppressed phases.

Although stratiform rain is not the dominant rain type in the enhanced phase, it contributes more to the total rainfall in the enhanced phase than it does in the suppressed phase. Stratiform rainfall accounts for 17% of the total rainfall in the enhanced phase and only 5% in the suppressed phase (Fig. 4c and 4d). The increase in total rainfall from the suppressed phase to the enhanced phase is due to an increase in stratiform rainfall.

In comparison to the enhanced phase, deep convection dominates total rainfall in the suppressed phase diurnal cycle, which contributes to 58% of the total rainfall throughout the day (Fig. 4d). Similarly to the enhanced phase, the suppressed phase has an early morning maximum in rainfall around 0100 LST. Even though deep convection prevails throughout the diurnal cycle, it contributes less to rainfall during the morning hours than it does in the afternoon. The morning peak in rainfall has a strong presence from deep convection and mixed precipitation with stratiform rainfall becoming more prevalent as the peak declines. Isolated convection contributes the most during the afternoon hours with deep convection taking over as the afternoon hours progress. Overall, isolated convection contributes more to the total rainfall in the suppressed phase; it contributes to 19% of the total rainfall in the suppressed phase and only 9% in the enhanced phase (Fig. 4c and 4d).

d. Diurnal cycle by MJO events

The mean diurnal cycle of rainfall separated by MJO events and MJO phases is plotted for TOGA radar (Fig. 5). There are large differences between the two events of the MJO enhanced phase, predominantly during the afternoon and morning hours that had rainfall maximums in the mean diurnal cycle (Fig. 5a, Fig. 4a). The first MJO event in October had significantly more overall rainfall than the second event in November. The afternoon maximum is largely attributed to data collected by the first MJO event. MJO event 2 has two small rainfall peaks at 1100 LST and 1800 LST. The MJO events in the suppressed phase are more similar than the two events of the enhanced phase. The two suppressed phase events observed around the same amount of rainfall throughout the diurnal cycle. Both events experienced a nocturnal peak between the hours of 2300 and 0500 LST. Both events experienced a minimum in precipitation around 0900 LST.

4. Discussion

The TOGA radar observed the diurnal cycle of rainfall that has distinct characteristics from the S-PolKa radar observed in Sakaeda et al. (2018). The mean diurnal cycle during the study period observed a strong morning peak in rainfall and a secondary afternoon peak from TOGA (Fig. 3). The morning maximum evolves from deep convective and mixed precipitation into stratiform rainfall as

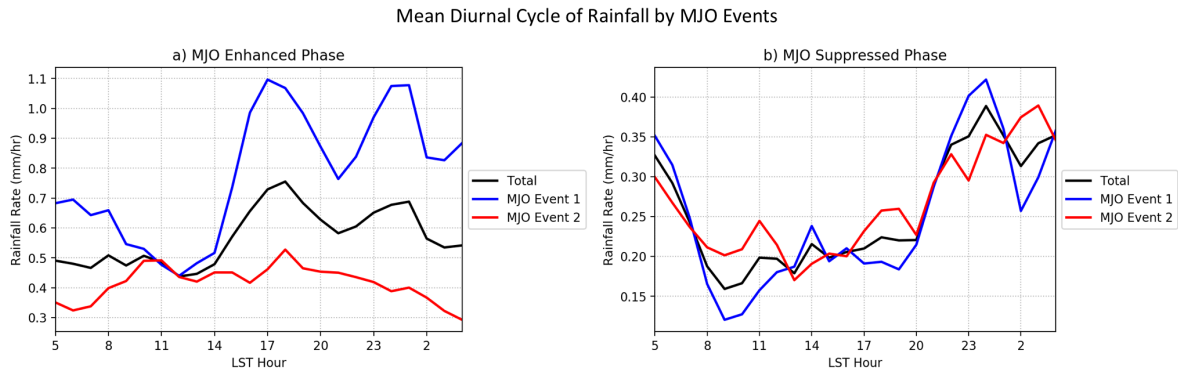


FIG. 5. Mean diurnal cycle of rainfall separated by MJO events and (a) MJO enhanced and (b) suppressed phases. The black line represents the total rainfall for the two MJO events, the blue line represents the rainfall for the first MJO event, and the red line represents the rainfall for the second MJO event.

documented by Sakaeda et al. (2018); this indicates the growth of convective cells into organized convective systems. The afternoon peak evolves in rain type from isolated convection into deep convection and mixed precipitation; this suggests the intensification of convective cells or the triggering of new cells from the outflow of previous cells. Comparing TOGA and S-PolKa, S-PolKa only observed an early morning peak during the entire diurnal cycle. S-PolKa experienced an early morning peak in rainfall during the enhanced phase and an early morning peak and secondary afternoon peak in the suppressed phase (Sakaeda et al. 2018). On the other hand, TOGA observed a pronounced afternoon maximum and lesser morning peak during the enhanced phase and only a morning peak in the suppressed phase (Fig. 4a and 4b). The large differences between the two MJO enhanced phase events could be skewing the results to see an afternoon peak in the overall diurnal cycle that was not present in Sakaeda et al. (2018) (Fig. 5a and 3). More suppressed phase days were observed and analyzed in this study that saw an afternoon peak; this could also contribute to the overall diurnal cycle observing an afternoon peak (Table 2).

Reasons for the differences between the diurnal cycle observed by the S-PolKa and TOGA radars remain to be explored further in future studies. Kerns and Chen (2018) found that the TOGA radar demonstrated a stronger afternoon maximum in diurnal rainfall than the other radars in the equatorial regions (such as S-PolKa) and also an earlier morning peak. The earlier morning peak happened around 2200 LST for TOGA and not until 0200 LST for S-PolKa (Fig. 3, Kerns and Chen 2018). Another study by Rowe et al. (2019) suggested there are 2-4 day periods of rain events within the MJO enhanced phases. The study suggests a dominant early morning peak in rainfall is observed during the rain event periods, but sometimes an afternoon peak is exhibited in the non-rain event periods. This is a speculation of why this study noticed a significant afternoon peak in the diurnal cycle of the enhanced phase

especially when analyzing major differences between the two MJO enhanced phase events (Fig. 5a). Future work should separate the TOGA radars MJO enhanced phases into these 2-4 day rain events to see if the same results can be replicated using this notion.

There are a number of factors that could have led to the observed differences between the S-PolKa and TOGA radars. The TOGA and S-PolKa radars have different wavelengths of measurement and were also at different locations. The DYNAMO field campaign took place during a La Niña year which could have affected sea surface temperatures more at TOGA than S-PolKa since TOGA was around 800 km east of S-PolKa (Xu and Rutledge 2014). This study did not examine potential impacts of sea surface temperatures. Future work analyzing SST may explain why the afternoon peak was so prominent at TOGA. Analysis of winds at the surface may also provide insight into the differences observed at each radar. One radar could have experienced stronger surface convergence or divergence within the enhanced or suppressed phases that influenced convection and the rainfall amounts observed. Limited sampling of two MJO events and limited domains for data collection are inevitable impacts influencing the results. It is also difficult to completely separate synoptic conditions such as equatorial Rossby waves to analyze only the MJO.

5. Conclusion

This research investigates the diurnal cycle of tropical rainfall and different rain types using data from TOGA radar during the DYNAMO field campaign. The field campaign aimed to examine MJO initiation processes and cloud evolution in order to improve prediction of the MJO. Composite analyses were applied to examine the daily rainfall rate, the mean diurnal cycle during the entire study period, the mean diurnal cycle during MJO enhanced and

suppressed phases, and the diurnal cycle during each MJO event. The major results from this research are as follows:

1. During the overall study period, a stronger afternoon peak in rainfall was observed when compared to the climatological diurnal cycle for a longer period of time over the tropical ocean.
2. Rainfall amounts increased from the MJO suppressed to enhanced phase due to an increase in stratiform rain.
3. A stronger afternoon maximum in rainfall was observed during the MJO enhanced phase than suppressed phase which differs from observations by S-PolKa radar.

Future work should investigate sea surface temperatures, surface winds, and the effects of rain events inside the MJO enhanced phases to better understand the differences between the diurnal cycles of S-PolKa and TOGA (Sakaeda et al. 2018; Rowe et al. 2019). The diurnal cycle is still not fully understood and further investigation into the diurnal cycle of the TOGA radar will increase the knowledge of MJO fundamentals.

Acknowledgments. This study was supported by Grant No. AGS-1560419 from the National Science Foundation. The statements and findings are those of the authors and do not necessarily reflect the views of the National Science Foundation. A special thanks is due to the mentor for this project, Dr. Naoko Sakaeda, for providing insight and guidance throughout this research process. The author would like to thank Dr. Daphne LaDue and the National Weather Center Research Experience for Undergraduates for hosting this program. The author would also like to thank Melanie Schroers, Andrew Berrington, and Briana Lynch for offering encouragement and coding support during this REU program.

References

- Gottschalck, J., 2014: What is the mjo, and why do we care? <https://www.climate.gov/news-features/blogs/enso/what-mjo-and-why-do-we-care>.
- Gottschalck, J., P. E. Roundy, C. J. Schreck III, A. Vintzileos, and C. Zhang, 2013: Large-scale atmospheric and oceanic conditions during the 201112 dynamo field campaign. *Monthly Weather Review*, **141** (12), 4173–4196, doi:10.1175/MWR-D-13-00022.1, URL <https://doi.org/10.1175/MWR-D-13-00022.1>, <https://doi.org/10.1175/MWR-D-13-00022.1>.
- Kerns, B. W., and S. S. Chen, 2018: Diurnal cycle of precipitation and cloud clusters in the mjo and itcz over the indian ocean. *Journal of Geophysical Research: Atmospheres*, **123** (18), 10,140–10,161, doi:10.1029/2018JD028589, URL <https://agupubs.onlinelibrary.wiley.com/doi/abs/10.1029/2018JD028589>, <https://agupubs.onlinelibrary.wiley.com/doi/pdf/10.1029/2018JD028589>.
- Madden, R. A., and P. R. Julian, 1971: Detection of a 4050 day oscillation in the zonal wind in the tropical pacific. *Journal of the Atmospheric Sciences*, **28** (5), 702–708, doi:10.1175/1520-0469(1971)028<0702:DOADOI>2.0.CO;2, URL [https://doi.org/10.1175/1520-0469\(1971\)028<0702:DOADOI>2.0.CO;2](https://doi.org/10.1175/1520-0469(1971)028<0702:DOADOI>2.0.CO;2), [https://doi.org/10.1175/1520-0469\(1971\)028<0702:DOADOI>2.0.CO;2](https://doi.org/10.1175/1520-0469(1971)028<0702:DOADOI>2.0.CO;2).
- Oh, J.-H., K.-Y. Kim, and G.-H. Lim, 2012: Impact of mjo on the diurnal cycle of rainfall over the western maritime continent in the austral summer. *Climate Dynamics*, **38** (5), 1167–1180, doi:10.1007/s00382-011-1237-4, URL <https://doi.org/10.1007/s00382-011-1237-4>.
- Powell, S. W., R. A. Houze, and S. R. Brodzik, 2016: Rainfall-type categorization of radar echoes using polar coordinate reflectivity data. *Journal of Atmospheric and Oceanic Technology*, **33** (3), 523–538, doi:10.1175/JTECH-D-15-0135.1, URL <https://doi.org/10.1175/JTECH-D-15-0135.1>, <https://doi.org/10.1175/JTECH-D-15-0135.1>.
- Powell, S. W., and R. A. Houze Jr., 2013: The cloud population and onset of the madden-julian oscillation over the indian ocean during dynamo-amie. *Journal of Geophysical Research: Atmospheres*, **118** (21), 11,979–11,995, doi:10.1002/2013JD020421, URL <https://agupubs.onlinelibrary.wiley.com/doi/abs/10.1002/2013JD020421>, <https://agupubs.onlinelibrary.wiley.com/doi/pdf/10.1002/2013JD020421>.
- Rockwell, A., 2012: Dynamo education and outreach summary. https://www.eol.ucar.edu/system/files/files/field_project/DYNAMO/DYNAMO_EO_Summary.f.pdf.
- Rowe, A. K., R. A. Houze Jr, S. Brodzik, and M. D. Zuluaga, 2019: The diurnal and microphysical characteristics of mjo rain events during dynamo. *Journal of the Atmospheric Sciences*, **76** (7), 1975–1988, doi:10.1175/JAS-D-18-0316.1, URL <https://doi.org/10.1175/JAS-D-18-0316.1>, <https://doi.org/10.1175/JAS-D-18-0316.1>.
- Sakaeda, N., G. Kiladis, and J. Dias, 2017: The diurnal cycle of tropical cloudiness and rainfall associated with the maddenjulian oscillation. *Journal of Climate*, **30** (11), 3999–4020, doi:10.1175/JCLI-D-16-0788.1, URL <https://doi.org/10.1175/JCLI-D-16-0788.1>, <https://doi.org/10.1175/JCLI-D-16-0788.1>.
- Sakaeda, N., S. W. Powell, J. Dias, and G. N. Kiladis, 2018: The diurnal variability of precipitating cloud populations during dynamo. *Journal of the Atmospheric Sciences*, **75** (4), 1307–1326, doi:10.1175/JAS-D-17-0312.1, URL <https://doi.org/10.1175/JAS-D-17-0312.1>, <https://doi.org/10.1175/JAS-D-17-0312.1>.
- Xu, W., and S. A. Rutledge, 2014: Convective characteristics of the maddenjulian oscillation over the central indian ocean observed by shipborne radar during dynamo. *Journal of the Atmospheric Sciences*, **71** (8), 2859–2877, doi:10.1175/JAS-D-13-0372.1, URL <https://doi.org/10.1175/JAS-D-13-0372.1>, <https://doi.org/10.1175/JAS-D-13-0372.1>.
- Yoneyama, K., C. Zhang, and C. N. Long, 2013: Tracking pulses of the maddenjulian oscillation. *Bulletin of the American Meteorological Society*, **94** (12), 1871–1891, doi:10.1175/BAMS-D-12-00157.1, URL <https://doi.org/10.1175/BAMS-D-12-00157.1>, <https://doi.org/10.1175/BAMS-D-12-00157.1>.
- Zhang, C., 2005: Madden-julian oscillation. *Reviews of Geophysics*, **43** (2), doi:10.1029/2004RG000158, URL <https://agupubs.onlinelibrary.wiley.com/doi/abs/10.1029/2004RG000158>, <https://agupubs.onlinelibrary.wiley.com/doi/pdf/10.1029/2004RG000158>.